

Experimental observation of photoresonance in electrons above a solid hydrogen surface

V. V. Zav'yalov and I. I. Smol'yaninov

Institute for Physical Problems, Academy of Sciences of the USSR

(Submitted 21 July 1986)

Zh. Eksp. Teor. Fiz. **92**, 339-349 (January 1987)

An experiment is described for observing the 1 → 2 and 1 → 3 photoresonance transitions in the spectrum of electrons over a solid hydrogen surface. The transition frequency is found to depend strongly on the pressure of the hydrogen vapor. If this dependence, which can be regarded as a manifestation of "quantum refraction" (multiple scattering), is interpreted on the basis of existing theory, the resulting scattering length for electron- H_2 scattering differs from the generally accepted value. In the limit of zero hydrogen vapor density, the measured frequency for the 1 → 2 transition is found to be 3.15 ± 0.05 THz. This yields an estimate 3.5 ± 0.3 eV for the height of the potential barrier for electrons above a solid hydrogen surface.

Most of the experimental and theoretical work on electron states over dielectric surfaces has been done for the case of liquid helium,¹ and relatively little is known for other dielectrics. In the simplest model, the interaction potential ϕ for an electron interacting with the dielectric surface depends only on the electrostatic images forces and on the external electric field \mathcal{E} , which is normal to the surface and is necessary experimentally in order to confine the electrons near the surface:

$$\begin{aligned} \phi(z) &= -\frac{e^2(\epsilon-1)}{4z(\epsilon+1)} + e\mathcal{E}z = -\frac{Qe^2}{z} + e\mathcal{E}z \quad \text{for } z > 0, \\ \phi(z) &= V_0 \quad \text{for } z \leq 0. \end{aligned} \quad (1)$$

Here ϵ is the dielectric constant of the surface, e is the elementary charge, and the z axis is normal to the surface. Solving the Schrödinger equation with this potential and letting $V_0 \rightarrow \infty$, one obtains the electron energy spectrum

$$E_n = -\frac{Q^2 m e^4}{2\hbar^2 n^2} + e\mathcal{E}\langle z_n \rangle + \frac{p_{||}^2}{2m}. \quad (2)$$

The first term in this expression gives the exact solution for $\mathcal{E} = 0$, while the second term gives the first-order correction for a nonzero confining field. The average distance from the electrons in the n th energy level to the surface is $\langle z_n \rangle = 3n^2\hbar^2/(2me^2Q)$. The last term in (2) corresponds to free electron motion parallel to the surface.

Similar electron states may exist over other (non-helium) dielectrics. Indeed, two-dimensional conduction was observed in Refs. 2 and 3, where the electron mobility was measured above liquid hydrogen, solid hydrogen, and solid neon surfaces. However, direct spectroscopic confirmation of a discrete electron spectrum above a dielectric surface has thus far been achieved only for helium.

The electron spectrum over a hydrogen surface is of particular interest, since it has been suggested by Khaikin⁴ that massive negative hydrogen ions may be present in the interstellar medium.

In this paper we report the observation of resonant light absorption involving the 1 → 2 and 1 → 3 spectral transitions for electrons confined over a solid hydrogen surface. The spectroscopic measurements were carried out at wavelengths 79, 84.3, and 107.7 μm by using a water-vapor laser,

and the electron spectrum was perturbed by changing the confining field \mathcal{E} .

As expected, the above simple model gives much poorer results for hydrogen than for helium. In addition, the energy levels were observed to depend strongly on the hydrogen vapor pressure. This dependence may be attributed qualitatively to "quantum refraction" (multiple scattering),^{5,6} an effect which has hitherto not been observed for two-dimensional electron systems.

EXPERIMENTAL APPARATUS

The experimental chamber for growing the crystalline hydrogen specimen (Fig. 1) was a thin-walled (0.2 mm) stainless steel cylinder with a heavy copper cover (1) and a copper ring, into which a 5-mm-thick single-crystal sapphire base (2) of diameter 35 mm was cemented. Sapphire was used because of its extremely large thermal conductivity, which is comparable to that for high-quality copper at the experimental temperatures. The chamber was placed inside an evacuated optical cryostat and thermally shielded from

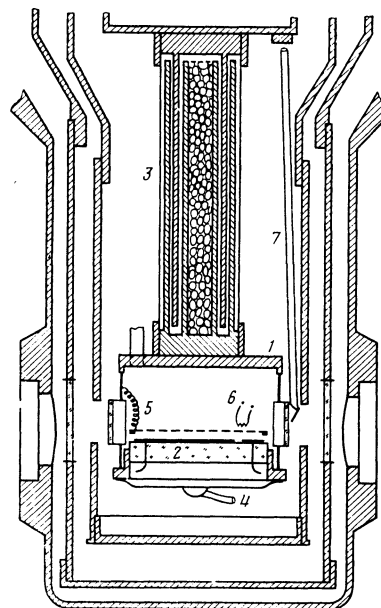


FIG. 1. Sketch of the optical cryostat.

the warm outer walls of the cryostat by two copper screens connected to nitrogen and helium reservoirs, respectively.

The chamber was equipped with disk-shaped single-crystal quartz optical windows 11 mm in diameter and 0.5 mm thick. The windows were vacuum-sealed by using sty-cast-1266 cement to glue them into thin-walled (~ 0.1 mm) cylindrical mountings soldered into the chamber walls. The cold windows in the nitrogen screen were made from 2-mm-thick sapphire single crystal, while 1-mm-thick single-crystal quartz was used for the warm vacuum windows.

The chamber cover was attached to the helium reservoir of the cryostat by means of an automatic thermal switch 3 (Fig. 1) consisting of three coaxial copper cylinders housed in a thin-walled hermetic stainless steel shell. The spacing between the cylinders was equal to 0.75 mm, and the heat-exchanging area was 21 cm². The inner cavity of the switch was filled with brand CaX zeolyte, and the switch was filled with the heat-exchanging gas (hydrogen) to a pressure of several torr at room temperature. When the chamber cooled down almost to the triple-point temperature for hydrogen, the hydrogen in the switch froze out and there was no further heat transfer (the switch turned off). During the remainder of the cooling process, the chamber exchanged heat with the helium reservoir only through its base, by means of a copper heat-exchanger 4 (20 cm long, 2.2 mm² cross section; Fig. 1). A constantan coil wound around the base ring regulated the temperature in the chamber.

We used technical-grade hydrogen in the experiments, which was purified by passage through a carbon adsorber (cooled to liquid nitrogen temperatures) and stored in a 6-liter metal booster tank. The latter was connected to the cryostat by a sylvon bellows, in which the pressure was measured by an MAS-31 vacuum meter to within ± 1 torr. Hydrogen was supplied to the cryostat by a thin-walled stainless steel tube in good thermal contact with the nitrogen reservoir of the cryostat. After the hydrogen crystallized in the chamber, the flow of gas in the tube was small enough so that the pressure difference between its ends was negligible.

Two electrodes 5 (Fig. 1) produced the uniform electric field used to confine the electrons over the hydrogen surface. The upper electrode (2.3 mm above the sapphire base) was grounded and in electrical contact with the chamber. The lower (aluminum) electrode was deposited on the sapphire by vacuum sputtering. A high voltage adjustable from 0 to 4 kV was fed to the lower electrode through two leads imbedded in the sapphire.

The measurements were made by slightly modulating the potential of the lower electrode at 8 kHz. The modulation signal reached the electrode through an isolating transformer.

The experimental configuration required that the upper electrode be transparent to the laser radiation probing the crystalline hydrogen surface. We therefore employed a grid electrode (grid period 0.5 mm) consisting of parallel copper wires of diameter 50 μ m mounted on a ring-shaped frame. A calculation showed that the field was uniform to within 0.1% halfway between the electrodes (i.e., at the hydrogen surface). The electrodes were 30 mm in diameter and were large enough so that the fringe fields could be neglected near the center of the laser-probed hydrogen surface.

The electrons injected toward the hydrogen surface were produced by a tungsten wire 10 μ m in diameter and 2

mm long, which served as the thermal emitter 6 (Fig. 1) and was located immediately above the upper grid electrode to one side of the probing laser beam. The emitter was heated by a single voltage pulse of duration ~ 0.1 s from a manually operated generator.

The electron spectra over the hydrogen surface were analyzed by using a gas-discharge water-vapor laser operating at the wavelengths 78.4, 79.1, 118.6 μ m (H₂O) and 84.3, 107.7 μ m (D₂O). By tuning the laser cavity we were able to achieve both single- and multi-frequency lasing at these wavelengths. The laser radiation was linearly polarized by inserting a horizontal copper wire of diameter 20 μ m into the cavity. The noise component of the laser output was decreased to 0.05% by optimizing the composition of the H₂O + H₂ + He or D₂O + D₂ + He gas mixtures. The laser radiation was modulated at acoustic frequencies (modulation factor $m = 0.01$ –5%) by modulating the discharge current. This enabled us to calibrate the sensitivity of the measuring system. The apparatus and methods for monitoring the laser radiation are described in detail in Refs. 7 and 8.

The probing laser beam was focused and deflected by two polyethylene lenses (on- and off-axis, with focal lengths 29 cm and 10 cm, respectively). Because polyethylene has negligible dispersion at the experimental wavelengths, the lens system was achromatic and could be used at any of the laser wavelengths without further adjustment. The radiation reflected by the hydrogen surface entered a metal guide 7 (Fig. 1) and was directed toward a Ge: B photodetector mounted on the copper wall of the helium reservoir of the cryostat. The signal from the photodetector passed through a source repeater and a pickup signal compensation circuit, reached a narrow-band amplifier, and was detected by an SD-1 synchronous detector with a time constant of 1 s (Fig. 2).

The voltage sinewave used to modulate the external field at 8 kHz also served as the reference signal for the synchronous detector, whose output voltage was fed to the *Y* input of an *X, Y* plotter equipped with two recording pens. The *X* input received the dc component of the signal from a high-resistance voltage divider shunting the lower electrode in the chamber.

The entire system was tuned and calibrated by modulating the laser radiation in phase with the potential of the lower electrode.

To determine whether electrons were present above the hydrogen surface, we separated the lower electrode into two unequal parts by making a gap of width 0.5 mm along a chord at a distance of 10 mm from the center of the electrode. The two parts thus formed were connected in parallel to a superconducting *LC* circuit.

The resonance frequency of the *LC* circuit should be shifted and the *Q*-factor should drop when free electrons are present over the hydrogen surface near the gap. The components C_e , R_e , and C_e in the electron detector circuit (Fig. 2) model the effects of the surface electrons. For the surface electron densities typical in our experiment, we get the estimates $C_e \sim 1$ pF and $R_e \sim 1$ M Ω . The *Q*-factor of the loaded circuit is given by

$$Q_e = [Q_0^{-1} + \omega_0 C_e^2 R_e / C_0 (4 + \omega_0^2 C_e^2 R_e^2)]^{-1}, \quad (3)$$

where Q_0 and ω_0 are the *Q*-factor and resonance frequency of

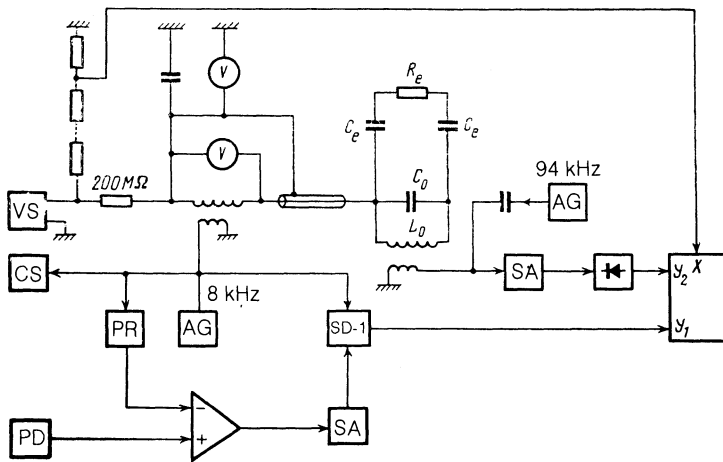


FIG. 2. Block diagram of the measurement system: VS, voltage source; AG, acoustic generator; SA, U2-8 selective amplifier; SD, synchronous detector; PD, photodetector; PR, phase rotator; CS, laser current stabilizer.

the circuit when no surface electrons are present. We see from (3) that the sensitivity is greatest when $\omega_0 C_e R_e \approx 2$ and increases with C_e/C_0 . We therefore selected an operating frequency of ~ 100 kHz. The resonant circuit was immersed in a liquid-helium chamber and surrounded by a superconducting lead shield. The inductor L_0 in the circuit consisted of 660 turns of niobium wire wound without using a core. Since the circuit was at the potential of the external confining field, the niobium coil was insulated by a Teflon spacer on which five turns of copper wire from the coupling coil were wound. A mica capacitor with $C_e = 270$ pF was used. The circuit Q (measured from the width of the resonance line) was $Q_0 \approx 1000$, and the natural frequency was $\nu_0 = 94$ kHz. The input signal from a GZ-102 oscillator was fed to the circuit through a capacitor $C_1 = 620$ pF. The output signal from the coupling coil passed through a narrow-band amplifier and was then detected and fed to the second (Y) input of the plotter. The oscillation amplitude in the circuit was generally ~ 0.5 V under our experimental conditions, and the amplitude of the rf electric field acting on the surface electrons was less than 2 V/cm. We verified that this field had no influence on the spectroscopic measurements even when the voltage across the circuit was increased 30-fold.

As an illustration, Fig. 3 shows a trace of the signal from the detector when the voltage U of the lower electrode in the chamber was scanned during the experiment. The successive changes are indicated by the arrows. When no free electrons were present near the surface, the signal was independent of

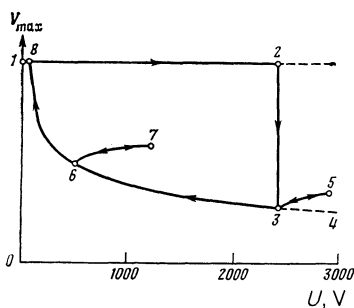


FIG. 3. Sample trace of signal from the electron detector recorded by scanning the voltage of the lower chamber electrode. The bottom portion 4-3-6-8 of the curve corresponds to irreversible escape of electrons from the hydrogen crystal surface. The sections 3-5 and 6-7 correspond to a reversible redistribution of the electrons on the surface.

U (Section 1-2). The drop in the signal (Section 2-3) at the instant the tungsten thermal emitter began to supply electrons testifies to the presence of free electrons above the surface. The bottom part of the curve (4-3-6-8) corresponds to complete screening of the static field well above the crystal surface by a charge of density

$$\sigma = -eU/4\pi h, \quad (4)$$

where h is the thickness of the hydrogen crystal and ϵ is its dielectric constant. Along this curve, the surface loses "excess" free electrons irreversibly as U decreases.

The behavior on Sections 3-5 and 6-7 is reversible as U changes, and the charge near the surface remains constant. The signal depends on U here because the surface charge redistributes itself reversibly, and the dependence becomes more pronounced as the sensitive gap of the detector moves closer to the edge of the base of the chamber. For each curve of the type 6-7, the surface charge density at the center was assumed to be equal to the value calculated by Eq. (4) for U at the bifurcation point (point 6).

EXPERIMENT

The hydrogen was crystallized from the liquid phase by cooling the base of the experimental chamber (the heater was turned off). The triple point for ordinary hydrogen lies at $P = 54$ torr and $T = 14.0$ K. After about 15 minutes, the solid/liquid interface floated to the top of the liquid and formed a mirror-like, meniscus-shaped surface. The solid hydrogen was optically transparent and probably consisted of several crystallites. During the remainder of the cooling process, the heater was turned on when the saturated vapor pressure decreased to 40 torr (which corresponds to $T = 13.4$ K) and the pressure was stabilized for roughly 1.5 h, during which time the meniscus disappeared and the surface of the crystal became smooth. We then applied a confining potential of 1-4 kV to the lower chamber electrode and pulsed the thermal emitter once to generate a burst of electrons toward the surface. We found that when the electrons were injected at pressures below 30 torr the surface acquired a stable bound charge, probably due to the high drift velocity of the electrons leaving the emitter. A bound charge also formed after repeated electron injections, even at high gas pressures. The bound charge was measured by an electron detector at the end of each experiment by recording the po-

tential required to completely remove the free charge from the surface (point 8 in Fig. 3). The bound charge, which can distort the field in the chamber, could be removed from the surface only by melting all the solid hydrogen in the chamber. In what follows we will discuss only the results obtained when no bound charge was present on the surface (so that points 1 and 8 coincided).

There was no significant escape of electrons from the hydrogen crystal surface when the latter was slowly cooled or heated (at rates below 2 K/h). More rapid temperature changes were accompanied by jumps in the signal from the electron detector which were associated with sudden leakage of electrons from the surface, probably due to cracking of the hydrogen crystal.

The tunable laser source enabled us to observe the photoresonance of the surface electrons when the electron spectrum was altered by changing the confining field \mathcal{E} . The latter is expressible in terms of the potential of the lower electrode by the formula

$$\mathcal{E} = [U - 4\pi\sigma(d - 2h)/(1 + \epsilon)] / [d - h(1 - 1/\epsilon)], \quad (5)$$

where d is the distance between the upper and lower electrode, σ is the surface charge density, and no bound charge is present. We measured U for several values of σ at photoresonance and used the results to deduce both the thickness h of the solid hydrogen crystal and the strength \mathcal{E}_{res} of the confining field corresponding to resonance. This method was used to find \mathcal{E}_{res} for the $1 \rightarrow 2$ resonance at the wavelengths 84.3 and 79 μm , for which the surface charge density could be varied over wide limits. The thickness thus obtained was used to find \mathcal{E}_{res} for the other transitions. The calculated values h agreed to within ± 0.1 mm with the average thickness measured directly by means of a cathetometer.

Figure 4 shows a typical experimental trace of the photoresonance signal at $\lambda = 84.3 \mu\text{m}$. We recall that in order to increase the sensitivity to $\sim 0.01\%$, we measured the absorption coefficient by recording a quantity which was proportional to the derivative of the absorption signal at the modulation frequency of the confining field. The traces show resonance transitions from the $n = 1$ to the $n = 2, 3$ states. The electrons absorbed $\sim 10^{-3}$ of the incident resonant radiation for the $1 \rightarrow 2$ transition and $\sim 10^{-4}$ for the $1 \rightarrow 3$ transition. The photoresonance signal amplitude depended linearly on the laser intensity and on the surface charge density.

Figure 5 shows the results from a calibration experi-

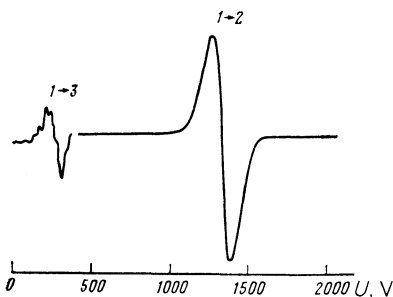


FIG. 4. Trace of the photoresonance signal recorded at $\lambda = 84.3 \mu\text{m}$ by scanning the potential of the lower electrode (hydrogen vapor pressure 40 torr). The $1 \rightarrow 2$ and $1 \rightarrow 3$ resonance transitions are clearly visible. The trace for the $1 \rightarrow 3$ transition was recorded at 2.5 times the sensitivity for the $1 \rightarrow 2$ transition.

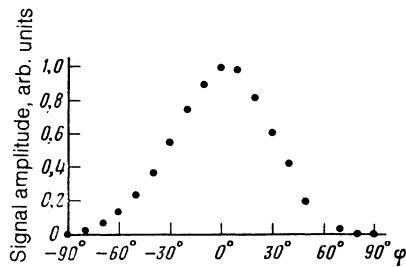


FIG. 5. Amplitude of the photoresonance signal (in arbitrary units) as a function of the orientation of the polarization vector for resonant, linearly polarized incident radiation. The signal is strongest when the polarization is perpendicular to the surface of the crystal.

ment in which we studied the dependence of the photoresonance signal amplitude on the polarization of the incident resonant radiation. The absorption coefficient for polarized radiation was greatest when the \mathbf{E} vector was perpendicular to the hydrogen surface; there was no absorption when \mathbf{E} was parallel to the surface. This result demonstrates the two-dimensional nature of the electron motion above the surface.

MEASUREMENTS

Figures 6–8 present the principal results of the measurements. Figure 6 shows \mathcal{E}_{res} for the $1 \rightarrow 2$ photoresonance transition as a function of the hydrogen vapor pressure over the solid surface for three laser wavelengths. We see that the experimental points lie on two curves, one of which is a replica of the other shifted along the vertical axis by an amount proportional to the laser frequency ν_{12} .

The curves $\nu_{12}(\mathcal{E}_{\text{res}})$ and $\nu_{13}(\mathcal{E}_{\text{res}})$ in Fig. 7 show the same measurements, supplemented by experimental data for the $1 \rightarrow 3$ transitions. Only those points corresponding to $P = 40$ torr for the $1 \rightarrow 2$ and $1 \rightarrow 3$ transitions and $P \rightarrow 0$ for the $1 \rightarrow 2$ transition are shown. The dashed lines show the position of the points corresponding to intermediate pressures.

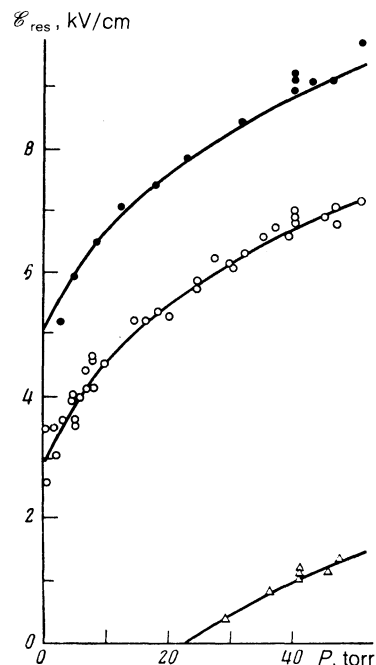


FIG. 6. Confining field \mathcal{E} at resonance versus hydrogen vapor pressure for three laser wavelengths: \bullet , 79; \circ , 84.3; \triangle , 107.7 μm .

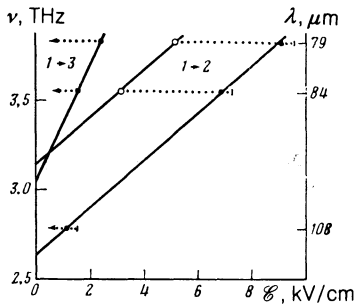


FIG. 7. Transition frequencies in the electron spectrum as a function of the confining electric field: ●, values measured for the 1→2 and 1→3 transitions, hydrogen pressure 40 torr; ○, values measured for the 1→2 transition at zero pressure.

Figure 8 plots the width $\Delta\nu$ of the resonance line for the 1→2 transition as a function of the pressure P ; $\Delta\nu$ was found by measuring the distance between the maximum and minimum of the photoresonance signal at $\lambda = 84 \mu\text{m}$. The data from Fig. 7 have been used to express the frequency scale along the vertical axis in terms of \mathcal{E}_{res} . We see that the results agree closely with the values found by measuring the rf mobility of electrons over solid hydrogen in Ref. 3.

We conclude from an analysis of the curves in Figs. 6 and 7 that (at least for the 1→2 transition) $d\nu/d\mathcal{E}_{\text{res}}$ is independent of P . This fact can be used to extrapolate the photoresonance frequencies to zero \mathcal{E} by recording their dependence on P . On the other hand, Eq. (2) shows that $d\nu_{12}/d\mathcal{E} = e[\langle z_2 \rangle - \langle z_1 \rangle]/2\pi\hbar$, whence the experimental values give $\langle z_2 \rangle - \langle z_1 \rangle = 64 \pm 4 \text{ \AA}$. A calculation based on the simplest model (Coulomb potential, hydrogen surface with an infinitely high barrier) gives the larger value 76 \AA . The corresponding experimental and calculated values for the 1→3 transition are $\langle z_3 \rangle - \langle z_1 \rangle = 160 \pm 20$ and 202 \AA , respectively.

The transition frequency when \mathcal{E} and P are equal to zero also differs greatly from the value calculated using the above model. The experimental frequency $\nu_{12}(0) = 3.15 \pm 0.05 \text{ THz}$ is 25% higher than the calculated value $\nu_{12}'(0) = 2.52 \text{ THz}$. The results of similar measurements for electrons over He^4 and He^3 (Refs. 9, 10) can be closely

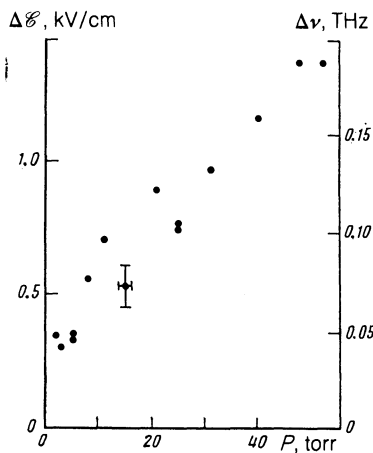


FIG. 8. Width of the 1→2 resonance line at $\lambda = 84.3 \mu\text{m}$ as a function of the hydrogen pressure (the dots show the linewidths at half-maximum, which are equal to $3^{1/2}$ times the distance between the extrema in the photoresonance signal).

approximated by introducing the Rydberg correction δ ; the energy spectrum is given by the formula

$$E_n = -Q^2 m e^4 / 2 \hbar^2 (n + \delta)^2, \quad (6)$$

where δ is independent of n . We thus find that $(\nu_{12}(0) - \nu_{12}'(0)) / \nu_{12}'(0) = -7\delta/3$. Measurements of δ for He^4 and He^3 give -0.022 and -0.014 , respectively, while for solid hydrogen we obtain $\delta = -0.11$.

The correction δ can be calculated for more realistic model potentials which allow for the finiteness of the potential barrier on the surface and truncate the Coulomb potential at interatomic distances.¹¹ For example, for the model potential

$$\varphi(z) = -Qe^2/z \quad \text{for } z \geq z_0, \quad \varphi(z) = -Qe^2/z_0 \quad \text{for } 0 < z < z_0, \\ \varphi(z) = V_0 \quad \text{for } z \leq 0$$

one obtains

$$\delta = 2\alpha / [a^* - 2\alpha \ln(z_0/a^*)], \quad (7)$$

where $\alpha^2 = \hbar^2 / (2mV_0)$ and $a^* = a_0/Q = 16.8 \text{ \AA}$ is the effective Bohr radius for an electron over a hydrogen surface. The barrier height is found to be

$$V_0 = \frac{2}{m} \left\{ \frac{\hbar}{a^* \delta} [1 - \delta \ln(z_0/a^*)] \right\}^2. \quad (8)$$

If we take the cutoff parameter z_0 equal to one or two times the lattice constant for the hydrogen crystal we get $V_0 \approx 3.5 \pm 0.3 \text{ eV}$, which agrees quite closely with the theoretical value 3.3 eV in Ref. 12. The agreement between the calculated and measured barrier heights V_0 for solid hydrogen is an important result, because the measured height $0.3 \pm 0.2 \text{ eV}$ for liquid hydrogen was found in Ref. 13 to differ greatly from the calculated value 2.2 eV .

For electrons over solid hydrogen the transition frequencies depend strongly on the hydrogen vapor pressure, and this is perhaps the most significant difference from the case of He^4 or He^3 surfaces. Figure 9 shows how the frequency of the 1→2 photoresonance transition (extrapolated to zero confining field) depends on the density N of H_2 in the vapor phase. The straightforward temperature-dependence

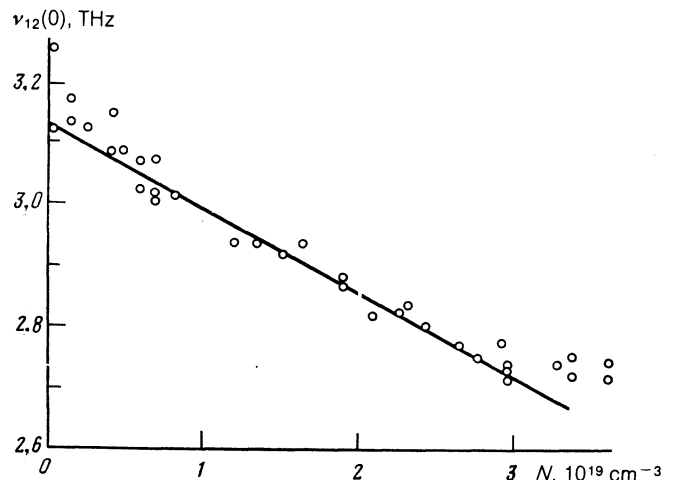


FIG. 9. Frequency of the 1→2 transition, extrapolated to zero confining field, as a function of the density of H_2 vapor molecules. The values have been corrected for the temperature dependence of the dielectric constant for solid hydrogen.

of the density (and hence the dielectric constant of the solid hydrogen) has been eliminated in Fig. 9 by introducing a correction which reaches 6% near the triple point for hydrogen. No correction is needed for the dielectric constant of the vapor over the solid hydrogen surface, since it was less than 1.0004 and was essentially constant at the experimental pressures.

At the triple point the average distance between the molecules in the vapor is $\approx 30 \text{ \AA}$, as compared with $\approx 100 \text{ \AA}$ at hydrogen vapor pressure $P = 1.5 \text{ torr}$. For comparison, the simplest model gives $\langle z_1 \rangle = 25 \text{ \AA}$ and $\langle z_2 \rangle = 101 \text{ \AA}$ for the average distance from the hydrogen surface to an electron in the first and second states, respectively. It is clear that under our conditions, the range of vapor pressures was such that almost no vapor molecules were present between ground-state electrons and the crystal surface, while many such molecules were present for electrons in the $n = 2$ state. The de Broglie wavelength for electrons along the surface was $\approx 300 \text{ \AA}$ at these temperatures.

A similar situation occurs in experiments on Rydberg atoms in a gas atmosphere¹⁴; the transition frequencies for the principal series with $n \gtrsim 20$ are again found to be shifted. This shift, which is linear in the gas pressure, was explained by Fermi,⁵ whose theory is developed, e.g., in Ref. 15. This effect (now referred to as quantum refraction) was predicted in Ref. 6 for electrons localized over liquid helium, but no experimental observations were reported.

According to the Fermi theory, the energy of an electron localized in a state of characteristic radius $r \gg N^{-1/3}$, where N is the density of gas molecules, is changed by an amount

$$\Delta E = 2\pi a \hbar^2 N / m. \quad (9)$$

The constant a is called the scattering length and is equal to the negative of the real part of the amplitude for s -scattering of an electron by a molecule. There is no correction to the energy if $r \ll N^{-1/3}$.

On the basis of the foregoing discussion, we can approximate the data in Fig. 9 by the formula

$$\nu_{12}(0) = \frac{Q^2 m e^4}{4\pi \hbar^3} \left[\frac{1}{(1+\delta)^2} - \frac{1}{(2+\delta)^2} \right] + \hbar a N / m. \quad (10)$$

For very low densities such that $\langle z_2 \rangle = 100 \text{ \AA} \ll N^{-1/3}$, $\nu_{12}(0)$ should be independent of N . However, our experiments failed to reveal such behavior. If our interpretation is correct, then the data imply that the scattering length for an electron by a hydrogen molecule is equal to $1.4 \pm 0.4 \text{ \AA}$. (The correction for the electric quadrupole moment of ortho-hydrogen lies within the $\pm 0.4 \text{ \AA}$ error.)

The shift in the transition frequencies for the Rydberg atoms Na, Rb, and Cs in a hydrogen atmosphere was studied in Ref. 16, and the scattering length in this case was found to be positive: $a = 0.54 \text{ \AA}$. However, these measurements were carried out at $T \sim 600 \text{ K}$, for which the molecular rotational states were highly excited and there was a large contribution from scattering involving states with nonzero moments.

The currently accepted value $a = 0.67 \text{ \AA}$ is found by extrapolating the measured cross section σ for $e\text{-}H_2$ collisions to the limit of zero collision energy, for which one has $\sigma = 4\pi a^2$. However, σ has been measured accurately only for energies above 20 meV (Ref. 17); σ was found to have a Ramsauer-Townsend dip at 9 meV in Ref. 18, but the cor-

rectness of these measurements is in doubt.¹⁹ Such a dip should occur if our value for a is correct.

The $e\text{-}H_2$ collision cross section can be found independently from our data on the photoresonance linewidths $\Delta\nu$ by using a Lorentzian function to approximate the resonance curve. The collision energy $\sim 1 \text{ meV}$ in this case lies in the thermal range. The corresponding formula, with allowance for the two-dimensional nature of the thermal motion on the surface, is¹

$$\sigma = 8\pi a^2 / 3\pi \hbar N \tau, \quad (11)$$

where

$$\tau = 1 / \pi \Delta\nu.$$

Substituting the values from Fig. 8, we find that $|a| = 1.3 \text{ \AA}$, in good agreement with the value calculated from the shift in the photoresonance frequency due to quantum refraction. The available data on σ do not suffice to determine the sign of the scattering length.

We note in closing that quantum refraction may also be important for electrons localized over deuterium or neon surfaces. We hope that the experiments now in progress along these lines will clarify the underlying physics and explain why our value of our scattering length a differs from the generally accepted result.

We are grateful to A. S. Borovik-Romanov for his interest in this work, to M. S. Khaikin for suggesting that we study this problem, and to V. C. Edel'man and E. P. Bashkin for helpful discussions.

¹V. S. Edel'man, Usp. Fiz. Nauk **130**, 675 (1980) [Sov. Phys. Usp. (1980)].

²A. M. Troyanovskii, A. P. Volodin, and M. S. Khaikin, Pis'ma Zh. Eksp. Teor. Fiz. **29**, 65, 421 (1979) [JETP Lett. **29**, 59, 382 (1979)].

³A. M. Troyanovskii and M. S. Khaikin, Zh. Eksp. Teor. Fiz. **81**, 398 (1981) [Sov. Phys. JETP **54**, 214 (1981)].

⁴M. S. Khaikin, Pis'ma Zh. Eksp. Teor. Fiz. **27**, 706 (1978) [JETP Lett. **27**, 668 (1978)].

⁵E. Fermi, Nuovo Cimento, II, 157 (1943); E. Fermi, Collected Works [Russian translation], Vol. 1, Nauka, Moscow (1971), p. 611.

⁶E. P. Bashkin, Zh. Eksp. Teor. Fiz. **82**, 1868 (1982) [Sov. Phys. JETP **55**, 1076 (1982)].

⁷V. V. Vav'yalov and G. D. Bogomolov, Prib. Tekh. Eksp., No. 3, 174 (1982).

⁸G. D. Bogomolov, V. I. Voronin, V. V. Zav'yalov, and I. N. Parfenov, Prib. Tekh. Eksp., No. 4, 187 (1973).

⁹C. C. Grimes, T. R. Brown, M. L. Burns, and C. L. Zipfel, Phys. Rev. **13**, 140 (1976).

¹⁰A. P. Volodin and V. S. Edel'man, Pis'ma Zh. Eksp. Teor. Fiz. **30**, 668 (1979) [JETP Lett. **30**, 633 (1979)].

¹¹T. M. Sanders and G. Weinreich, Phys. Rev. B **13**, 4810 (1976).

¹²M. W. Cole, Phys. Rev. **2**, 4239 (1970).

¹³B. Halpern and R. Gomer, J. Chem. Phys. **51**, 1031 (1969).

¹⁴S. Chen and M. Takeo, Rev. J. Mod. Phys. **29**, 20 (1957).

¹⁵V. A. Alekseev and I. I. Sobel'man, Zh. Eksp. Teor. Fiz. **49**, 1274 (1965) [Sov. Phys. JETP **22**, 882 (1965)].

¹⁶T. Z. Ny and S. Y. Chen, Phys., Rev. **54**, 1045 (1938).

¹⁷S. Trajmar, D. F. Register, and A. Chutjian, Phys. Rep. **97**, 221 (1983).

¹⁸G. R. Freeman and T. Wada, Bull. Amer. Phys. Soc. **24**, 1114 (1980).

¹⁹R. W. Crompton and M. A. Morrison, Phys. Rev. A **26**, 3695 (1982).

Translated by A. Mason